

The Lepton Flavor Changing Decays and One-loop Muon Anomalous Magnetic Moment in the Extended Mirror Twin Higgs Models

Guo-Li Liu^{1,*}, Fei Wang^{1,†}, Wenyu Wang^{2,‡}

¹ *School of Physics and Microelectronics,*

Zhengzhou University, Zhengzhou, 450001, China

² *Institute of Theoretical Physics, Faculty of Science,*

Beijing University of Technology, Beijing 100124, China

Abstract

Mirror Twin Higgs(MTH) models always contain heavy gauge bosons and extra Higgses. Besides, to accommodate tiny neutrino masses via seesaw mechanism, new heavy neutrinos can also be introduced in MTH extension models. Such new particles and interactions may lead to new contributions to the lepton flavor violating (LFV) processes, including $\ell_i \rightarrow \ell_j \gamma$ and $\ell_i \rightarrow \ell_j \ell_k \ell_l$. We find that current experimental data can stringently constrain the parameter spaces and certain LFV processes can possibly be tested by the next generation colliders. One-loop contributions of the new particles to the muon anomalous magnetic momentum are also calculated. Such contributions can still not solve the discrepancy between the experiments and the prediction of the standard model.

PACS numbers: 13.38.Dg,14.66.-z,12.60.-i

* guoliliu@zzu.edu.cn

† feiwang@zzu.edu.cn

‡ wywang@bjut.edu.cn

I. INTRODUCTION

In the Standard Model (SM), the conservation of individual lepton flavor numbers and the presentation of the GIM mechanism [1] guarantee that the LFV processes in the SM are tiny. For example, the SM prediction of the branch ratio $BR_{SM}(l_j \rightarrow l_i \gamma) \sim 10^{-55}$ [2] is very small, which would never be probed at the colliders. Therefore, it will be an obvious evidence of new physics beyond the SM if we observe any signature of the LFV processes in future experiments, so LFV processes are very efficient in exploring new physics beyond the SM. As the upper bounds of the LFV processes by current experiments have been given with impressive accuracy, it is interesting to explore whether theoretical predictions of a typical new physics model can agree with the experimental results.

Many works have been completed to look for the LFV processes $l_i \rightarrow l_j \gamma$, $l_i \rightarrow l_j l_k l_l$ in new physics models, see e.g. [3–15]. At the same time, additional interactions involving the leptons may contribute to the muon anomalous magnetic momentum. The presence of additional contributions to $g_\mu - 2$ are welcome to solve the discrepancy between the theoretical predictions of SM and the experiments. Therefore, it is well motivated to see if the anomaly can be solved in various new physics models [16–21].

It is well known that the neutrino oscillation experiments [22–30] indicate that neutrinos possess tiny masses and can convert into each other. So individual lepton flavor numbers $L_i = L_e, L_\mu, L_\tau$ may be violated at the electroweak scale. Weinberg’s effective dimension-5 operator is the lowest one that can generate tiny Majorana-type neutrino masses. Such an operator can be ultraviolet(UV)-completed to obtain three types of tree-level seesaw mechanism: type I seesaw [31], involving the exchange of right-handed neutrinos; type II seesaw [32], involving the exchange of scalar triplet; type III [33], involving the exchange of fermion triplet. The neutrino seesaw mechanisms can also be embedded into various well motivated new physics models to accommodate the neutrino masses, such as the Mirror Twin Higgs (MTH) model [34].

MTH, which extends the SM with a mirror copy, can stabilize the Higgs mass from quadratic divergent quantum corrections by a discrete mirror symmetry. The new particles, which are related to the SM particles by this discrete symmetry, do not carry the SM color charge and can hardly be produced and detected at the colliders, ameliorating the stringent constraints on the mass of the top partner by the Large Hadron Collider(LHC) [35].

Although MTH is theoretically appealing, it encounters difficulties by cosmological considerations. In the simplest realization of MTH [34] model, the twin particles will eventually transfer their entropies into twin photons and twin neutrinos, which behave as extra radiation components and contribute to the expansion of the Universe. We know that the SM neutrinos will contribute to the effective degrees of freedom N_{eff} by an amount $N_{eff} \sim 3.046$ [36, 37]. In the MTH model, the Twin photons and Twin neutrinos, which are the extra relativistic species, increase the SM prediction by an additional amount $\Delta N_{eff} \sim 5.6$ [38]. However, Big bang nucleosynthesis(BBN), anisotropies in the cosmic microwave background (CMB) by the Planck 2018 constrained $N_{eff} \sim 3$ [39, 40], which challenges MTH.

Various modifications are proposed to reduce the N_{eff} value and solve the problems of MTH. For example, the first and second generations of twin fermions as well as twin photon can be absent [41]. The twin neutrinos can also be heavy [42, 43]. In certain circumstances, even the Twin photon can be heavy without affecting naturalness [44, 45]. Asymmetric entropy production can be possible after the Twin and SM sectors decouple [38, 43, 46, 47].

In the seesaw extension models of MTH, extra massive right-handed neutrinos in both sectors can be introduced to generate tiny neutrino masses. Typical lepton-flavor-changing couplings may naturally appear in this mechanism, which can lead to interesting phenomenological consequences and possibly constrain some parameters in this model. Besides, as new interactions involving the leptons may contribute to the muon anomalous magnetic momentum, it is interesting to see if the discrepancy on the $g_\mu - 2$ anomaly can be ameliorated in this model. Therefore, we will study the LFV processes $\ell_i \rightarrow \ell_j \gamma$, $\ell_i \rightarrow \ell_j \ell_k \ell_l$ and the muon anomalous magnetic moment a_μ at the one-loop level in this work.

The paper is organized as follows. In section II, the MTH model will be extended to include new LFV couplings. We will discuss the new structures and the effective couplings. One-loop contributions to the muon anomalous magnetic moment a_μ will be calculated in section III. In section IV, the amplitudes and the branching ratios of rare LFV processes $\ell_i \rightarrow \ell_j \gamma$, $\ell_i \rightarrow \ell_j \ell_k \ell_l$ will be calculated, respectively. The corresponding numerical results are also given. Section V summarizes and concludes the whole work.

II. THE MTH MODELS AND THE LEPTON FLAVOR CHANGING COUPLINGS

A. The general discussion of the model and the LFV couplings

In the MTH framework, the particle contents include two parts: the SM particles and its mirror copy of all the SM fields. The SM particles and the mirror sectors are related by the discrete Z_2 twin symmetry. The global symmetry of the Higgs sector in the simplest realization can be taken to be $SU(4) \times U(1)$. Both the global symmetry and the discrete symmetry are approximate. The global symmetry contains the SM electroweak gauge symmetries and twin gauge symmetries. The pseudo-Nambu-Goldstone bosons (pNGBs), which arises from the spontaneously breaking of the the global $SU(4) \times U(1)$ symmetry to $SU(3) \times U(1)$, contain the SM Higgs doublet. The Higgs mass, under the joint action of the global symmetry and the discrete twin symmetry, are protected from one loop quadratic divergence.

As noted previously, additional contributions to N_{eff} of MTH will cause difficulties in cosmology¹. One can impose another portal, such as the neutrino portal to reduce the N_{eff} to the acceptable level. Meanwhile, new flavor-changing couplings can be generated via the mixing between the SM neutrino and the Twin neutrino [48],

$$\begin{aligned} \mathcal{L}_{\text{int}(\nu, \tilde{\nu})} = & \frac{g}{\sqrt{2}} \bar{\ell} \gamma^\mu P_L (c_\theta \nu + s_\theta \tilde{\nu}) W_\mu^+ + \text{h.c.} \\ & + \frac{g}{2c_w} (c_\theta \bar{\nu} + s_\theta \tilde{\bar{\nu}}) \gamma^\mu P_L (c_\theta \nu + s_\theta \tilde{\nu}) Z_\mu, \end{aligned} \quad (1)$$

where $c_\theta = \cos \theta$, $s_\theta = \sin \theta$. Here θ is the mixing angle between ordinary neutrino and twin neutrino. The LFV couplings in Eq.(1) can origin from typical neutrino seesaw extension of MTH model via introducing the massive right-handed neutrino [49],

$$\mathcal{L} \supset -y_{ij} (L_A^i H_A N_A^j + L_B^i H_B N_B^j) - \frac{1}{2} (M_N)_{ij} (N_A^i N_A^j + N_B^i N_B^j) - (M_{AB})_{ij} N_A^i N_B^j, \quad (2)$$

in both the SM and twin sectors. The Weinberg dimension-5 operator, which was used in some references (such as Ref. [50]), can be generated by integrating out the heavy right-handed neutrinos.

¹ In scenarios with multiple dark matter components, small contributions to N_{eff} can possibly solve the discrepancy between the value of H_0 extracted from local measurements versus CMB data.

B. The general form of the LFV couplings in the MTH models

The new particles, which induce the LFV couplings, could be new gauge bosons Z_μ^H , new scalars H^0, H^\pm and N_H species of heavy neutrinos $\nu_{H,i}$. The general forms of the LFV couplings from the effective Lagrangian of leptonic sector [51, 52] can be summarized as ²

$$\begin{aligned} \mathcal{L} \supseteq & \frac{g_2}{\sqrt{2}} \sum_{i=1}^{4N_g-3} \sum_{j=1}^3 V_{ji}^* \bar{\nu}_{H,i} \gamma^\mu W_\mu P_L \ell_j + y_{l_j} \sum_{i=1}^{N_h} \sum_{j=1}^3 U_{ji}^* \bar{\nu}_{H,i} H^+ P_R \ell_j + h.c. \\ & + \lambda_\ell \bar{\ell} H^0 \ell + g_\ell \bar{\ell} \gamma^\mu Z_\mu^H P_L \ell + \lambda_{ji} \bar{\ell}_i H^0 \ell_j + \sum_{i \neq j} g_{ji} \bar{\ell}_i \gamma^\mu Z_\mu^H (f_v + f_a \gamma^5) \ell_j + h.c. \end{aligned} \quad (3)$$

Here g_ℓ , λ_ℓ are the couplings of the heavy neutral gauge boson and the scalar to the charged lepton, respectively. The coefficients g_{ji} , λ_{ji} are the couplings between different lepton flavors. We consider both the vector type (f_v) and the axial-vector (f_a) type couplings of Z_μ^H to different flavor generations.

The first term of eqn.(3) is a generalization of eqn.(1) from typical neutrino seesaw extension of MTH model. In general, the neutrino mass matrix M will involve the left-handed neutrinos, the right-handed neutrinos and their twin neutrino partners, which will be a $4N_g \times 4N_g$ matrix for N_g generation of neutrino species. The matrix M is arranged so as that its upper-left 3×3 submatrix of M denotes the ordinary Pontecorvo-Maki-Nakagawa-Sakata (PMNS) [53, 54] neutrino mixing matrix. The flavor changing couplings V_{ji} , which is just the M_{nm} matrix element of the most general $4N_g \times 4N_g$ unitary neutrino mixing matrix M with $1 \leq n \leq 3$ and $4 \leq m \leq 4N_g$, also characterize the deviation of the PMNS matrix to unitary. It can be estimated to be $\sum_j |V_{ji}|^2 \lesssim 1 - \sum_{i=1}^3 |U_{Li}|^2 \lesssim 0.01$ with $L = e, \mu, \tau$ [52, 55]. As noted in [48], the "two seesaw" scenario with type-I seesaw in both the SM and mirror sector can not induce large mixing between SM neutrino and heavy mirror neutrino. The "SM seesaw, Dirac twin neutrinos" scenario can possibly induce large mixing to reduce the twin sector's contribution to the radiation density. The sum of the heavy neutrinos in the first term of eqn.(3) can be understood to be dominated by the mirror $\tilde{\nu}_R$ parts in this

² The gauge couplings involving heavy neutrino $\nu_{H,i}$ can arise from the couplings of the form $\bar{\nu}_{i,L} \gamma^\mu W_\mu l_{j,L}$. The left-handed neutrino, which is the interaction eigenstate, can be written as the combination of mass eigenstates involving the light and heavy neutrinos. We do not include in the Lagrangian the terms involving the SM-like light neutrinos and keep only the new contributions involving heavy neutrinos from typical neutrino mass generation mechanisms. Similar discussions can be given for the Yukawa-type interactions with $\nu_{H,i}$.

scenario. We will not specify the nature of the heavy neutrinos in our following discussions and only adopt their upper bounds in our numerical calculations.

The second term of eqn.(3) with extended Higgs sector can appear in certain composite Twin Higgs models. The coupling can be decomposed as the production of $y_i = m_{l_i}/\sqrt{2}v$ and U_{ij} , with the matrix U_{ij} contains V_{ji} and the mixing between ordinary Higgs and exotic Higgs. In this work, we will also take them as free parameters.

III. ONE-LOOP CONTRIBUTION TO THE MUON ANOMALOUS MAGNETIC MOMENT

The Brookhaven National Laboratory [56] had measured the anomalous magnetic moment of the muon

$$a_\mu^{\text{exp}} = 11659208.0(6.3) \times 10^{-10}, \quad (4)$$

which has a 3.3σ to 3.6σ deviation from the prediction of the SM [57, 58]

$$\Delta a_\mu = a_\mu^{\text{exp}} - a_\mu^{\text{SM}} = (28.3 \pm 8.7 \text{ to } 28.7 \pm 8.0) \times 10^{-10}. \quad (5)$$

From the couplings of Eq. (3), one can easily calculate the new contributions to the muon anomalous magnetic moment which are generated by one loop diagrams involving the exchange of W_μ gauge boson/charged scalar H^\pm and heavy neutrino, or Z_μ^H gauge boson and muon, or H^0 neutral scalar and muon, as shown in Fig.(1).

Note that the contributions from Fig.(1)(e)(f) contain self energy of the fermions, which will disappear due to the electromagnetic gauge invariance.

We can define a_μ^{TH} as

$$a_\mu^{TH} = a_\mu^{\nu W} + a_\mu^{\nu H} + a_\mu^{Z^0} + a_\mu^{H^0}. \quad (6)$$

The contribution to muon anomalous magnetic moment a_μ involving W and the massive neutrino loop (see Fig.1a) can be written as

$$a_\mu^{\nu W} \simeq \frac{V_\mu^2 e m_\mu}{64\pi^2 m_W^4} \sum_{k=1}^3 V_{\mu k}^* V_{\mu k} m_{\nu_k}^2. \quad (7)$$

The contribution to a_μ involving the charged Higgs H^\pm and the heavy neutrino loops (see Fig.1(b)) can be written as

$$a_\mu^{\nu H} \simeq -\frac{y_\mu^2 e m_\mu}{32\pi^2 m_{H^\pm}^4} \frac{5}{6} \sum_{k=1}^3 U_{\mu k}^* U_{\mu k} m_{\nu_k}^2. \quad (8)$$

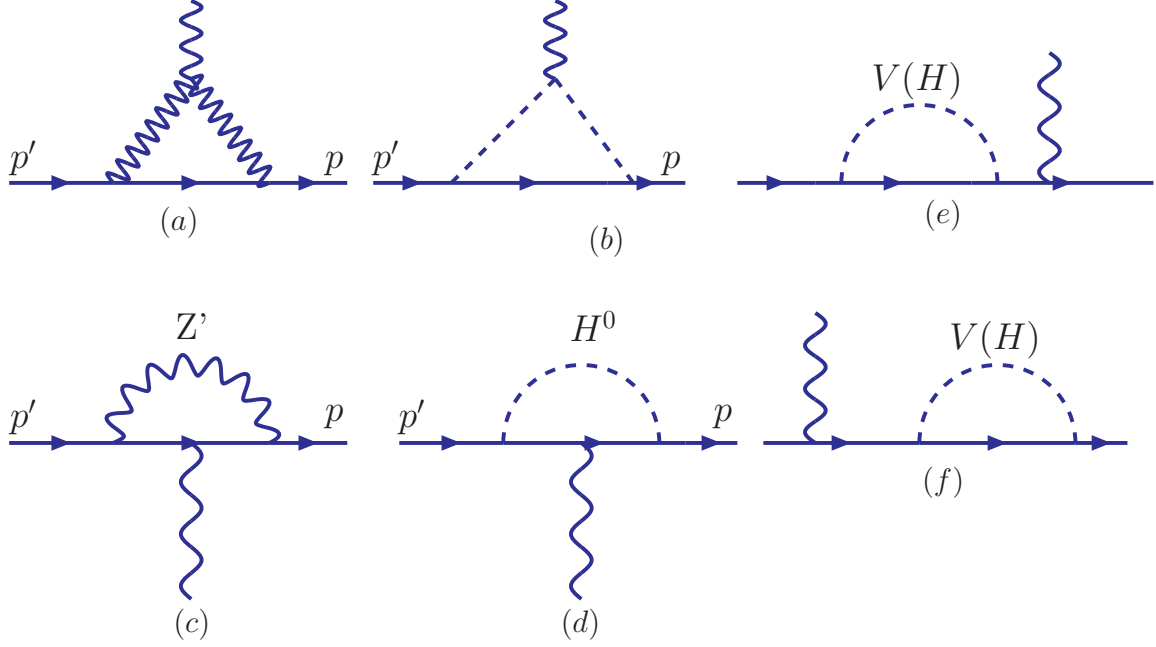


FIG. 1: The triangle and the penguin type diagrams for the muon anomalous magnetic moment at the one-loop level (with both the final and the initial particles being muons) and the decays $\ell_i \rightarrow \ell_j \gamma$ (with the final state fermion line being ℓ_j and the initial state line being ℓ_i).

We should note that the contribution involving the charged Higgs H^\pm and the light neutrino loops are much smaller than this contribution for not very small $m_{\nu,H}$.

The contribution to a_μ involving Z^H (see Fig.1(c)) can be written as [52]

$$a_\mu^{Z^0} = \frac{g_\mu^2}{4\pi^2} \frac{m_\mu^2}{M_{Z^0}^2} \bullet \frac{1}{3}. \quad (9)$$

Finally, the contribution to a_μ involving the extra Higgs can be given by [52]

$$a_\mu^{H^0} = \frac{\lambda_\mu^2}{32\pi^2} \frac{2m_\mu^2}{m_{H^0}^2} \bullet \frac{2}{3}. \quad (10)$$

We can estimate the contributions of these four terms. If we assume that the heavy neutrinos are degenerate with $m_1 = m_2 = m_3 = m_{\nu,H}$, the term $\sum_{k=1}^3 V_{\mu k}^* V_{\mu k} m_{\nu_{H,k}}^2$ in $a_\mu^{\nu W}$ can be estimated to be $m_{\nu,H}^2 \sum_{k=1}^3 |V_{\mu k}|^2 \lesssim 0.01 m_{H,\nu}^2$. Similarly, $\sum_{k=1}^3 U_{\mu k}^* U_{\mu k} m_{\nu_k}^2$ can be estimated to be less than $0.01 m_{H,\nu}^2 \sin^2 \zeta$, with ζ the mixing between ordinary Higgs and exotic Higgs. The couplings can be given as $y_l = m_l/v$ and $em_\mu/(64\pi^2) \sim 5.4 \times 10^{-5}$, respectively. If we take $m_{H^\pm} \sim 300 \text{ GeV}$ and the mixing angle $\sin \zeta \lesssim 0.01$, the contributions $a_\mu^{\nu W}$ and $a_\mu^{\nu H}$ can be estimated to be $4.6 \times 10^{-20} m_\nu^2$ and $0.57 \times 10^{-20} m_\nu^2$, respectively. Thus the

magnitude of the contributions depend on the mass scale of the heavy neutrino mass $m_{\nu,H}$, which should be larger than 10^5 TeV for them to account for the discrepancy (see Eq.(5)). However, too large mass of the heavy (mirror right-handed like) neutrino will induce large mirror Z_2 breaking, reintroducing quadratic sensitivity to the cutoff scale into the Higgs mass term. With very large neutrino mass, the contributions of the charged gauge boson and the charged Higgs at one-loop level can still not possibly account for the discrepancy between the experiments and the theoretical predictions, which can be seen in Fig.2(a). So we will not take such a heavy neutrino.

We can fix the following mass parameters $m_{\nu} = 2000$ GeV, $m_{H^+} = 300$ GeV and vary the one-loop muon anomalous magnetic moment with the mixing parameters V_{μ} and y_{μ} . The results given in Fig.2(b) also indicate that it is difficult to explain the discrepancy between the experiments and the theoretical prediction.

Since there is a minus sign before the charged scalar contribution to the muon anomalous magnetic moment, the curve of Fig.2(b) becomes flat, which can be explained by the formulae given in Eq.(7) and Eq.(8). Though there seems a large decline in the curve of a_{μ} verse mixing y_{μ} , the decline value of muon anomalous magnetic moment actually is quite small, from 1.38×10^{-11} to 1.2×10^{-11} .

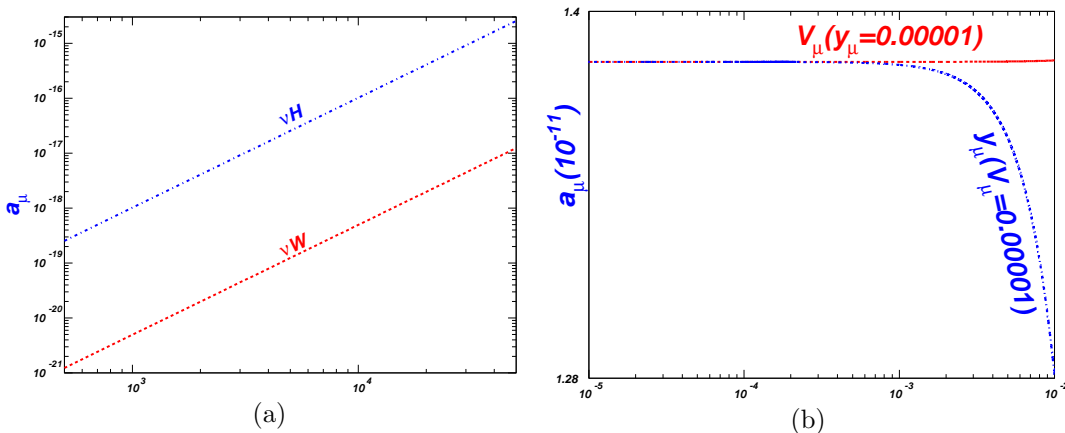


FIG. 2: The one-loop contributions of the LFV couplings to the the muon anomalous magnetic moment.

The contributions of the neutral gauge boson and the neutral Higgs to the muon anomalous magnetic moment are of order 1.02×10^{-10} and 5.7×10^{-10} , respectively, even with $g \sim \mathcal{O}(1)$, $\lambda \sim \mathcal{O}(1)$, $m_{Z_H^0} \sim 1TeV$ and $m_{H^0} \sim 300 GeV$. They are too small to account for

the discrepancy and can be neglected safely. Of course, the couplings can not be chosen to be $\mathcal{O}(1)$ with the suppression of the muon mass.

So we conclude from Fig.(2) that, as long as the heavy neutrino mass is not too large, the contributions of both the gauge bosons and the scalars to the one-loop muon anomalous magnetic moment can not account for the discrepancy.

IV. THE PROCESSES $\ell_i \rightarrow \ell_j \gamma$ AND $\ell_i \rightarrow \ell_j \ell_k \ell_l$

In this section, we analyze the branching ratios of certain LFV processes in the MTH model, including $\mu \rightarrow e \gamma$, $\tau \rightarrow e(\mu) \gamma$, $\mu \rightarrow 3e$, $\tau \rightarrow 3e$, $\tau \rightarrow 3\mu$.

A. The width and the Branching ratios of the rare decay $\ell_i \rightarrow \ell_j \gamma$

The Feynman diagrams for $\ell_i \rightarrow \ell_j \gamma$, which can be mediated by the gauge bosons, the neutral Higgs and the charged Higgs, are shown in Fig.1. The initial and the final leptons are ℓ_i and ℓ_j , respectively.

The effective amplitude of $\ell_i \rightarrow \ell_j \gamma$, which are mediated by the W and the massive neutrinos (corresponding to the Fig.1(a)), can be written as

$$M^{\nu W}(\ell_i \rightarrow \ell_j \gamma) \simeq \frac{ieV_\mu V_e^* m_i}{32\pi^2} \bullet \bar{u}(p)(C_{12} - 2C_{21} + 2C_{23})(1 + \gamma^5)[2(p' \cdot \epsilon)]u(p'). \quad (11)$$

where $C_{ij} = C_{ij}(p_\gamma, -p', m_i^2, m_j^2, m_{Z^0}^2(m_H^2))$ are the one-loop three point functions [59] and the final state lepton masses are neglected with $m_j = 0$.

Similarly, we can obtain the effective amplitude mediated by the charged Higgs H^\pm and the massive neutrinos (corresponding to the Fig.1(b))

$$M^{\nu H}(\ell_i \rightarrow \ell_j \gamma) \simeq \frac{iey_\mu y_e^* m_i}{32\pi^2} \bullet \bar{u}(p)(C_{21} - C_{23} + C_{11} - C_{12})(1 + \gamma^5)[2(p' \cdot \epsilon)]u(p'). \quad (12)$$

Similarly, the contribution of the heavy neutral Z_H^0 and the heavy Higgs H^0 to $\ell_i \rightarrow \ell_j \gamma$ can be written as

$$\begin{aligned} M^{Z_H^0}(\ell_i \rightarrow \ell_j \gamma) &= \frac{ieg_\mu g_{\mu e} m_i}{16\pi^2} \bullet \bar{u}(p)[2(f_a - f_v)(C_{22} - C_{23} - C_{12})P_R, \\ &\quad -4(f_v + f_a)C_{12}P_L][2(p' \cdot \epsilon)]u(p') \\ M^{H^0}(\ell_i \rightarrow \ell_j \gamma) &= \frac{-ie\lambda_\mu \lambda_{\mu e} m_i}{16\pi^2} (C_{22} - C_{23} - C_{12} - C_0) \bullet \bar{u}(p)[2(p' \cdot \epsilon)]u(p'), \end{aligned} \quad (13)$$

where f_v , f_a are the vector and the axial-vector coupling coefficients of the heavy neutral gauge boson to leptons, respectively.

So the total amplitude can be given as

$$\begin{aligned}
M_{total} &= M^{\nu W} + M^{\nu H} + M^{Z^0} + M^{H^0} \\
&= \bar{u}(p) \cdot \frac{ie m_i}{32\pi^2} \{ V_\mu V_{\mu e}^* (C_{12} - 2C_{21} + 2C_{23})(1 + \gamma^5) \\
&\quad + y_\mu y_{\mu e}^* (C_{21} - C_{23} + C_{11} - C_{12})(1 + \gamma^5) \\
&\quad + 2g_\mu g_{\mu e} [-2(f_v - f_a)(C_{22} - C_{23} - C_{12})P_R - 4(f_v + f_a)C_{12}P_L] \\
&\quad - 2\lambda_\mu \lambda_\mu (C_{22} - C_{23} - C_{12} - C_0) \} \cdot 2(p' \cdot \epsilon) u(p') \\
&= m_i \cdot \bar{u}(p) (A + B\gamma^5) \cdot 2(p' \cdot \epsilon) u(p'), \tag{14}
\end{aligned}$$

where

$$\begin{aligned}
A &= \frac{ie}{32\pi^2} \{ V_\mu V_{\mu e}^* (C_{12} - 2C_{21} + 2C_{23}) + y_\mu y_{\mu e}^* (C_{21} - C_{23} + C_{11} - C_{12}) \\
&\quad + 2g_\mu g_{\mu e} [-(f_v - f_a)(C_{22} - C_{23} - C_{12}) - 2(f_v + f_a)C_{12}] \\
&\quad - 2\lambda_\mu \lambda_{\mu e} (C_{22} - C_{23} - C_{12} - C_0) \}, \tag{15}
\end{aligned}$$

$$\begin{aligned}
B &= \frac{ie}{32\pi^2} \{ V_\mu V_{\mu e}^* (C_{12} - 2C_{21} + 2C_{23}) + y_\mu y_{\mu e}^* (C_{21} - C_{23} + C_{11} - C_{12}) \\
&\quad + 2g_\mu g_{\mu e} [-(f_v - f_a)(C_{22} - C_{23} - C_{12}) + 2(f_v + f_a)C_{12}] \}. \tag{16}
\end{aligned}$$

So, the decay width is given as

$$\Gamma(\ell_i \rightarrow \ell_j \gamma) = \frac{m_i^3}{8\pi} \cdot m_i^2 (|A|^2 + |B|^2) = \frac{m_i^5}{8\pi} (|A|^2 + |B|^2). \tag{17}$$

1. The process $\mu \rightarrow e\gamma$

The width of the dominant muon-decay mode $\mu \rightarrow e\nu\bar{\nu}$ is given as,

$$\Gamma^\mu = \Gamma(\mu \rightarrow e\nu\bar{\nu}) \simeq m_\mu^5 G_F^2 / (192\pi^3), \tag{18}$$

where $G_F = \frac{\sqrt{2}g^2}{8m_W^2}$ is the Fermi coupling constant. So the branching ratios of the rare decay $\mu \rightarrow e\gamma$ is given by

$$BR(\mu \rightarrow e\gamma) = \frac{\Gamma(\mu \rightarrow e\gamma)}{\Gamma(\mu \rightarrow e\nu\bar{\nu})} = \frac{24\pi^2}{G_F^2} (|A|^2 + |B|^2), \tag{19}$$

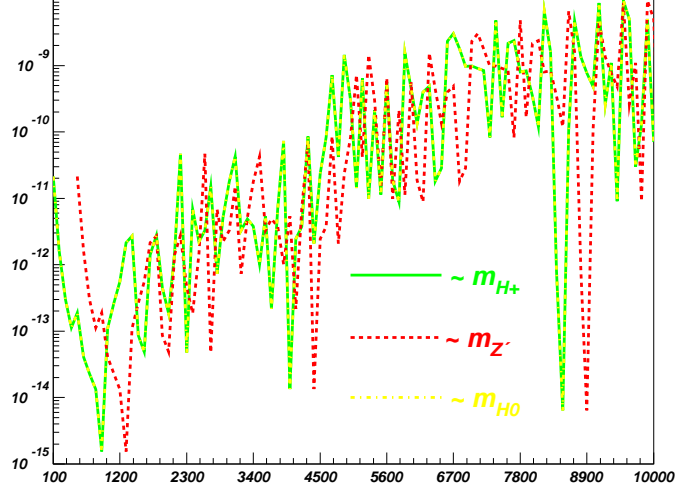


FIG. 3: With $V_{\mu e} = y_{\mu e} = g_{\mu e} = \lambda_{\mu e} = 10^{-5}$, the branching ratios of $\mu \rightarrow e\gamma$ versus parameters m_{H^\pm} , m_{Z^0} , m_{H^0} are plotted respectively.

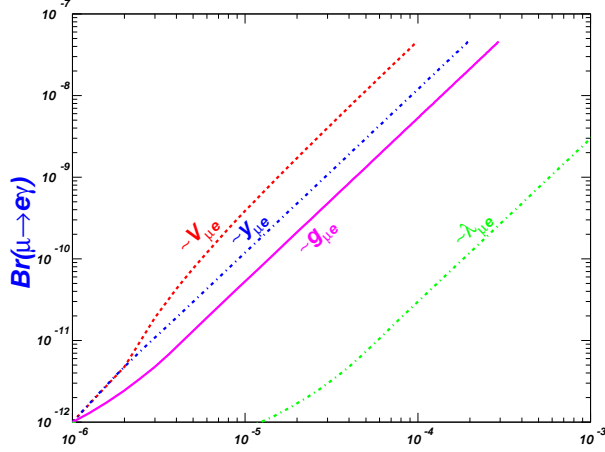


FIG. 4: With $m_{Z^0} = 1000 \text{ GeV}$, $m_\nu = 2000 \text{ GeV}$, $m_{H^\pm} = m_{H^0} = 300 \text{ GeV}$, the branching ratios of $\mu \rightarrow e\gamma$ versus parameters $V_{\mu e}$, $y_{\mu e}$, $g_{\mu e}$, $\lambda_{\mu e}$ are plotted respectively.

In Fig.(3), we show the contributions to the branch ratios from the new gauge bosons and the scalars, respectively. We can see that the dependence of the branch ratios on the various mass parameters are oscillatory in some ranges. So in the following discussions, we will take the fixed values for them: $m_{Z^0} = 1000 \text{ GeV}$, $m_{H^\pm} = m_{H^0} = 300 \text{ GeV}$, $m_\nu = 2 \text{ TeV}$.

In Fig.(4), we show the dependence of the branch ratios on the couplings, which increase monotonously along with the couplings. So the couplings can play a more important rule in controlling the branching ratios in comparison with the mass parameters. We will

concentrate mainly on the effects of the couplings in our following discussions.

The experimental upper bound is given by [60, 61]

$$BR(\mu \rightarrow e\gamma) < 4.2 \times 10^{-13}. \quad (20)$$

From this upper bound, the approximate range of the couplings can be given as

$$V_{\mu e} \geq 0.00145, \quad y_{\mu e} \geq 0.0035, \quad g_{\mu e} \geq 0.00003, \quad \lambda_{\mu e} \geq 0.0026, \quad (21)$$

for each type of contribution of new particle with fixed mass parameters.

Constraints in (21) for the couplings $V_{\mu e}$ and $y_{\mu e}$ are mild, given the electroweak coupling strengthen $\sim g/(2\sqrt{2})$. Constraints on the coupling $\lambda_{\mu e} \geq 0.0026$, however, is rather stringent because of the flavor changing suppression for the $H^0\mu\bar{e}$ couplings. As noted in [53], suppressed flavor mixing between μ and e is of order 10^{-5} , which is much smaller than the detectable limit. So, we will not discuss the contribution from the the neutral Higgs in our subsequent discussions.

Though $g_{\mu e}$ is also suppressed by the flavor changing mixing, the lower bound in (21) is mild and acceptable. So, still some parameter space for $g_{\mu e}$ can survive. Given that the branching ratio is also affected by the structure factors f_v, f_a , we will consider the effects of them in Fig.6. From the left panel of Fig.6, we can see that the branching ratios prefer large differences between f_v, f_a , which indicates that the left-handed coupling will give dominant contributions. To verify that, we scan the parameter space and show the points in the right part of Fig.6 with $g_{\mu e} = 0.00005$. It can be seen that possible ranges of f_v and f_a concentrate on different sides of the figures.

Actually, we also take into account the coherent terms and scan the possible ranges of the couplings. The contours of these couplings are shown in Fig.5. From the figures, we can see that larger $V_{\mu e}$ or $y_{\mu e}$ is favorable for the processes to be detected at the colliders.

2. The processes $\tau \rightarrow e\gamma$ and $\tau \rightarrow \mu\gamma$

As for the $\tau \rightarrow e\gamma$ and $\tau \rightarrow \mu\gamma$, the total width is different from that of the muon since the τ can decay not only into $e\nu\bar{\nu}$, but also into $\mu\nu\bar{\nu}$. Besides, it can decay hadronically since tau is heavier than the light quarks. Taking into account the unitarity of the quark mixing matrix, $|V_{ud}|^2 + |V_{us}|^2 = 1 - |V_{ub}|^2 \simeq 1$, one can easily get the lowest-order width

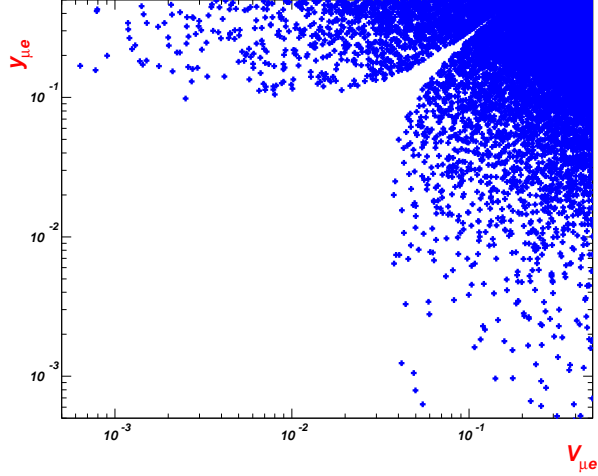


FIG. 5: With $m_{Z_H^0} = 1000 \text{ GeV}$, $m_\nu = 2000 \text{ GeV}$, $m_{H^\pm} = m_{H^0} = 300 \text{ GeV}$, the contour of $V_{\mu e}$ and $y_{\mu e}$ from the constraint of the branching ratios of $\mu \rightarrow e\gamma$.

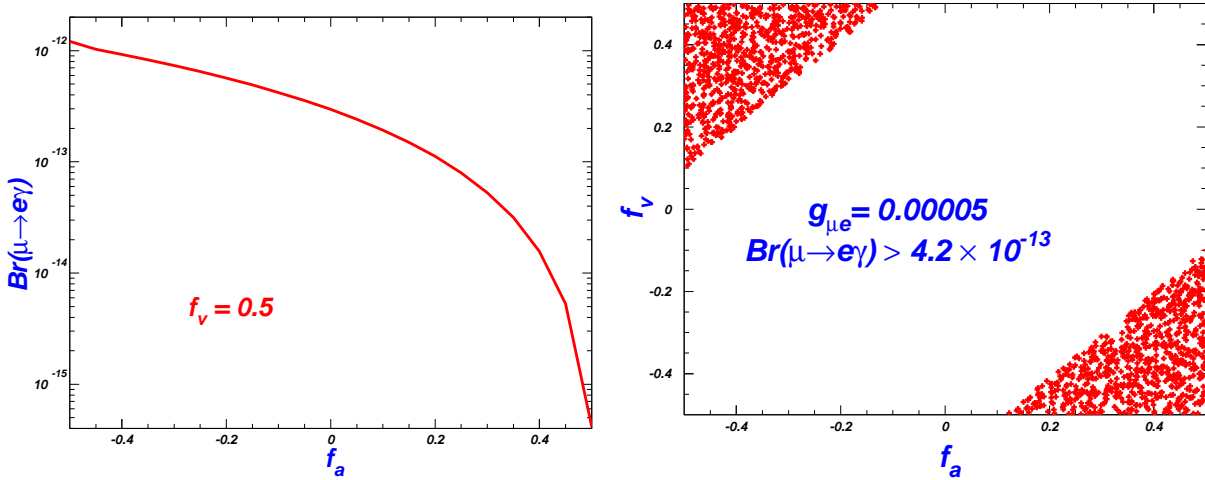


FIG. 6: With $m_{Z_H^0} = 1000 \text{ GeV}$ and $g_{\mu e} = 0.00005$. Left panel: $f_v = 0.5$, the contribution of the parameter f_a to the $\mu \rightarrow e\gamma$ branching ratio. Right panel: the scan the possible survivals of f_v , f_a in 10000 random points.

(see e.g. Ref. [62] and the Refs. in it),

$$\Gamma_{\tau;total} = \Gamma_\mu \frac{m_\tau^5}{m_\mu^5} [2 + N_C(|V_{ud}|^2 + |V_{us}|^2)] \simeq 5 \cdot \Gamma_\mu \frac{m_\tau^5}{m_\mu^5} \quad (22)$$

So the branching ratios of $\tau \rightarrow e\gamma$ and $\tau \rightarrow \mu\gamma$ can be written as,

$$BR(\tau \rightarrow e/\mu\gamma) = \frac{\Gamma(\tau \rightarrow e/\mu\gamma)}{\Gamma_{total}^\tau} = \frac{24\pi^2}{5G_F^2} (|A|^2 + |B|^2), \quad (23)$$

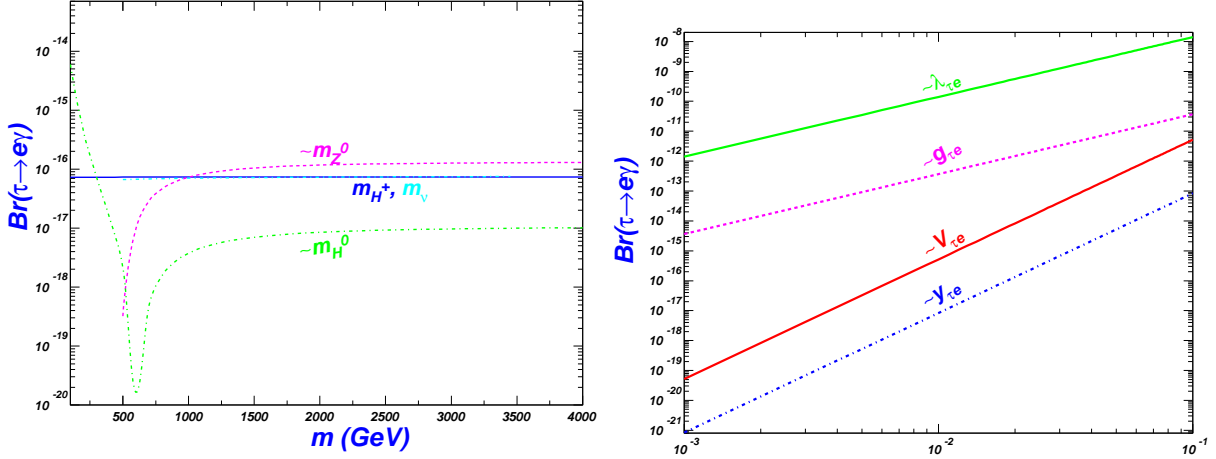


FIG. 7: With the couplings fixed $V_{\tau e} = y_{\tau e} = 0.01$, $g_{\tau e} = \lambda_{\tau e} = 0.00005$, the branching ratios of $\tau \rightarrow e\gamma$ versus parameters left: m_{H^\pm} , $m_{Z_H^0}$, m_{H^0} ; right: with $m_{Z_H^0} = 1000 \text{ GeV}$, $m_\nu = 2000 \text{ GeV}$, $m_{H^\pm} = m_{H^0} = 300 \text{ GeV}$, the constraints of the parameters $V_{\tau e}$, $y_{\tau e}$, $g_{\tau e}$, $\lambda_{\tau e}$ on the branching ratios of $\tau \rightarrow e\gamma$.

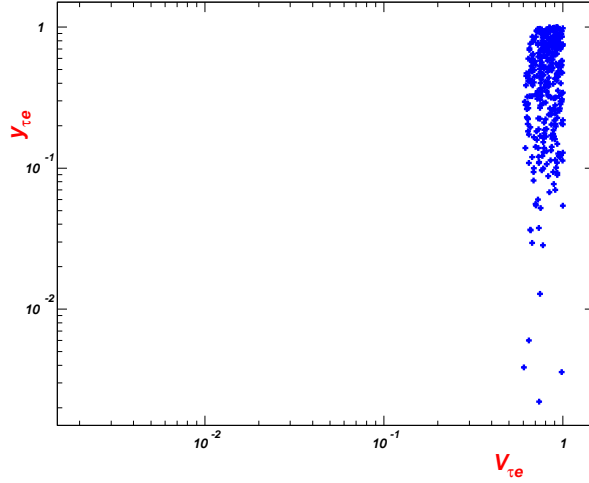


FIG. 8: With $m_{Z_H^0} = 1000 \text{ GeV}$, $m_\nu = 2000 \text{ GeV}$, $m_{H^\pm} = m_{H^0} = 300 \text{ GeV}$, the contour of $V_{\tau e}$ and $y_{\tau e}$ from the constraint of the branching ratios of $\tau \rightarrow e\gamma$.

The experimental upper bound are [63],

$$BR(\tau \rightarrow e\gamma) < 3.3 \times 10^{-8}, \quad BR(\tau \rightarrow \mu\gamma) < 4.4 \times 10^{-8}. \quad (24)$$

The LFV processes $\tau \rightarrow e\gamma$ and $\tau \rightarrow \mu\gamma$ can be discussed as follows. Since the final particle masses are neglected and the couplings are the same for the two processes, we only need to discuss the case $\tau \rightarrow e\gamma$.

In the left panel of Fig.7, we show the branching ratio of $\tau \rightarrow e\gamma$ from the contribution of the new gauge bosons and the scalars, respectively. It can be seen that the branching ratios are not sensitive to the change of the mass parameters for the charged gauge boson, the charged Higgs, and the heavy neutrino, respectively. In the region with lighter m , the neutral gauge boson and the Higgs can give large contributions with little suppression from the masses. On the other hand, in the heavier m region, the decay rates are almost independent on the m parameters and the curves are flat in their tails.

Numerical results indicate that the branching ratios of τ to $e\gamma$ shown in Fig.7 are smaller than those of μ . It can be understood as the following reasons. The branching ratios of τ to $e\gamma$ are not the same as those of μ because the τ lepton is about 17 times heavier than the μ lepton, corresponding to a much large y_τ . Moreover, the total width of τ lepton is 5 times larger than that of μ lepton.

The right panel of Fig.7 shows the dependence of the branching ratios on the various couplings. When $y_{\tau e}$ closes to 0.1, the branching ratio can reach the detectable sensitivity at the collider, as shown in (24). This range of coupling, however, is too large to be realistic.

So we can crudely draw a conclusion that the decay $\tau \rightarrow e\gamma$ (and $\tau \rightarrow \mu\gamma$) can hardly be detected at the collider. Even though this LFV process can hardly be detected, it is instructive to see the constraints of the branching ratio $\tau \rightarrow e\gamma$ on $V_{\tau e}$ and $y_{\tau e}$. We show in Fig.(8) the allowed values of the two parameters by the constraints in (24). It is clear from the figure that the branch ratio is not sensitive to $y_{\tau e}$ and large values of $V_{\tau e}$ can be allowed.

B. The decay $\mu \rightarrow 3e$ and $\tau \rightarrow \ell e^+ e^-$ ($\ell = e, \mu$)

1. *The decay $\mu \rightarrow 3e$ and $\tau \rightarrow 3e$ mediated by the neutral gauge bosons and the neutral scalar Higgs*

Since the mediator neutral gauge bosons are much heavier than the muon, the width of the three-body decay $\mu \rightarrow 3e$ via the neutral gauge bosons can be written as

$$\begin{aligned} \text{Br}(\mu^- \rightarrow e^- e^+ e^-) &= \frac{\Gamma(\mu^- \rightarrow e^- e^+ e^-)}{\Gamma(\mu^- \rightarrow e^- \nu \nu)} \\ &= \frac{\kappa \tilde{g}_{V\mu e}^2 \tilde{g}_{Vee}^2 / M_V^4}{\kappa g_W^4 / M_W^4} \\ &= \frac{\tilde{g}_{V\mu e}^2 \tilde{g}_{Vee}^2}{g_W^4} \frac{M_W^4}{M_V^4}, \end{aligned} \quad (25)$$

where $\tilde{g}_{V\mu e}^2 = |g_{V\mu e}^{(V)}|^2 + |g_{V\mu e}^{(A)}|^2$, $\tilde{g}_{ee}^2 = |g_{Vee}^{(V)}|^2 + |g_{Vee}^{(A)}|^2$. M_V is the mass of the gauge boson, κ is a kinematic-spin factor common to all decay modes mediated by the neutral vector boson, while g_W ($G_F/\sqrt{2} = g_W^2/(2M_W^2)$) and M_W are the electroweak coupling and the W boson mass, respectively.

So via the same idea, the three-body decay of the lepton τ involving vector mesons in the intermediate state can be written as

$$\begin{aligned} \text{Br}(\tau^- \rightarrow \ell^- e^+ e^-) &= \frac{\Gamma(\tau^- \rightarrow \ell^- e^+ e^-)}{\Gamma(\tau^- \rightarrow \ell^- \nu \nu)} \frac{\Gamma(\tau^- \rightarrow \ell^- \nu \nu)}{\Gamma(\tau^- \rightarrow \text{All})} \\ &= \frac{\Gamma(\tau^- \rightarrow \ell^- e^+ e^-)}{\Gamma(\tau^- \rightarrow \ell^- \nu \nu)} \frac{\Gamma(\tau^- \rightarrow \ell^- \nu \nu)}{\Gamma(\mu^- \rightarrow e^- \nu \nu)} \frac{\Gamma(\mu^- \rightarrow e^- \nu \nu)}{\Gamma(\tau^- \rightarrow \text{All})} \\ &= \frac{\tilde{g}_{V\tau \ell}^2 \tilde{g}_{Vee}^2}{g_W^4} \frac{M_W^4}{M_V^4} \left(\frac{M_\tau}{M_\mu}\right)^5 \frac{\Gamma_{total}^\mu}{\Gamma_{total}^\tau} \end{aligned} \quad (26)$$

Note that in the above formulas, the final lepton masses have been neglected.

The current 90% C.L. bounds on the above decay modes are [64, 65],

$$BR(\mu \rightarrow 3e) < 1.0 \times 10^{-12}, BR(\tau \rightarrow 3e(e\mu\mu)) < 2.7 \times 10^{-8}, BR(\tau \rightarrow 3\mu) < 2.1 \times 10^{-8}. \quad (27)$$

The dependence of the branching ratios on the parameters \tilde{g} and the mediator gauge boson mass m_V are given in Fig.10 for $\mu \rightarrow 3e$ and $\tau \rightarrow 3e$. We find that the branching ratios with our choice of parameters are much smaller than the experimental bounds Eq.(27) in most of the allowed parameter space. We can roughly estimate the upper bounds for the couplings $\tilde{g}_{\mu e}, \tilde{g}_{\tau e}$ to be

$$\tilde{g}_{\mu e} \leq 0.0018, \quad \tilde{g}_{\tau e} \leq 0.65, \quad (28)$$

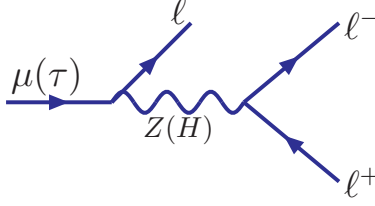


FIG. 9: The neutral boson contributions of the LFV couplings to the three final leptonic states of the second or the third generation lepton.

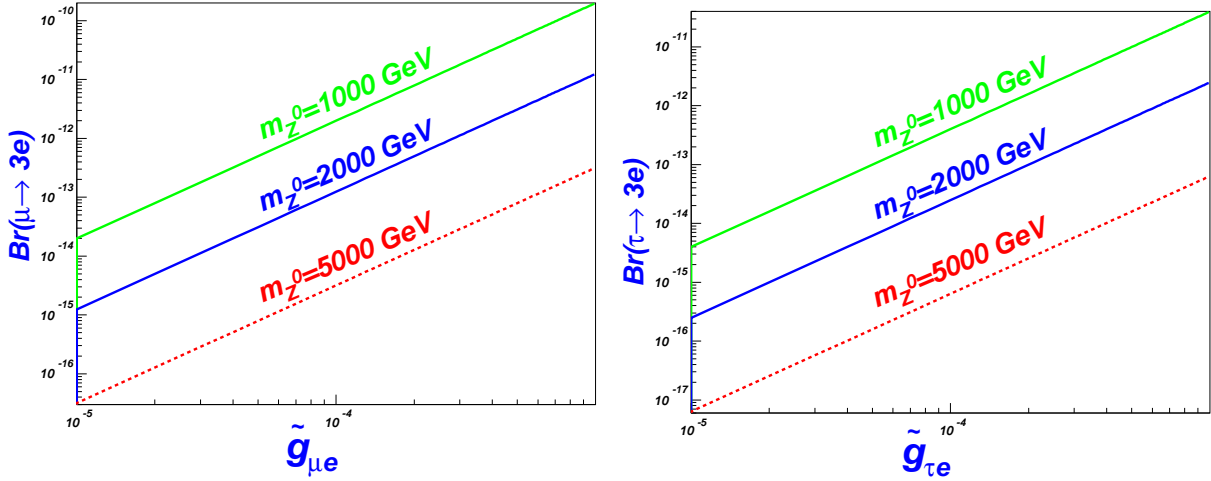


FIG. 10: The branching ratios of $\mu \rightarrow 3e$ (left) and $\tau \rightarrow 3e$ (right) versus parameters \tilde{g} for $m_{Z'_0} = 1000, 2000, 5000$ GeV, respectively.

with $M_V = 1000$ GeV.

Clearly, the neutral Higgs scalar mediated decay modes $\ell_i \rightarrow \ell_j \ell_j \ell_j$ are much smaller than that of the neutral Z'_0 gauge boson. The reason is that the Yukawa couplings are usually highly suppressed, i.e, m_τ/v , m_μ/v are much smaller than the gauge coupling g_W .

2. *The decay $\mu \rightarrow 3e$ and $\tau \rightarrow 3e$ mediated by the charged scalar Higgs and the right handed neutrino at the one-loop level*

Since there are no tree-level contributions to the $\ell_i \rightarrow \ell_j \ell_j \ell_j$ decay modes by the charged bosons and Higgs, some works, such as Refs. [66, 67], consider these processes at the one-loop level. We will reappear this with the flavor changing couplings mediated by the charged Higgs and the right-handed neutrino.

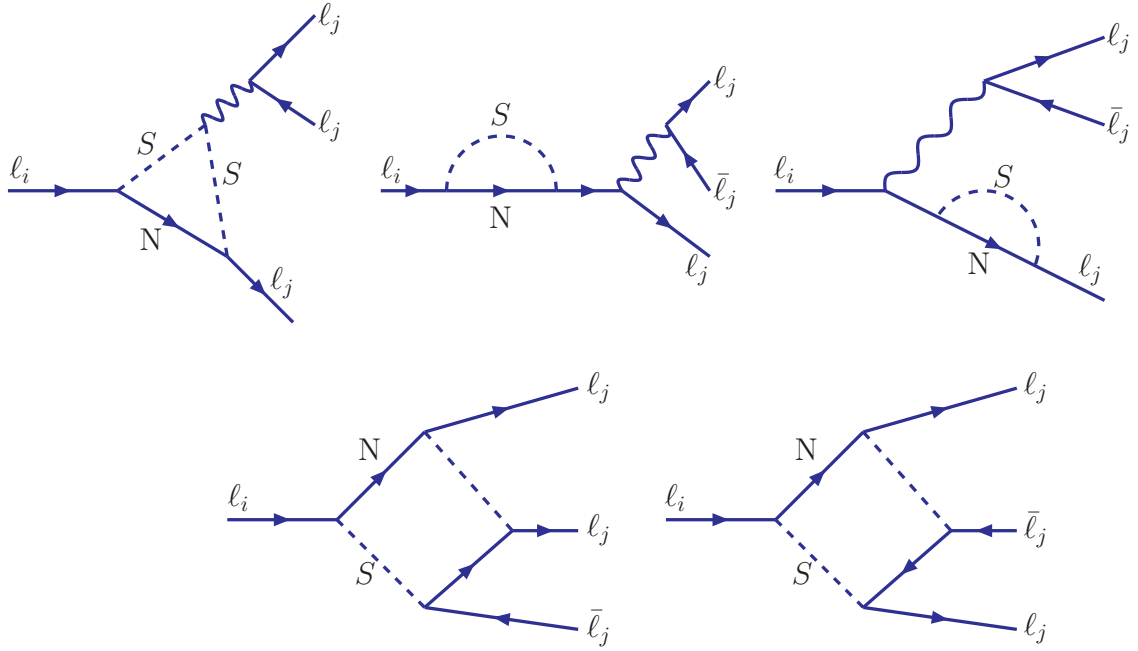


FIG. 11: The one-loop charged scalar contributions of the LFV couplings to the three final leptonic states of the second or the third generation lepton.

The couplings between the charged Higgs, the charged gauge bosons with the right-handed neutrinos and the charged leptons can induce the three-body decay of the massive charged leptons at one-loop level. Typical Feynman diagrams are shown in Fig.11 and the branching ratio[66, 67] can be written as

$$\begin{aligned}
\mathcal{B}^{(N)}(l_i \rightarrow l_j \bar{l}_j l_j) &= \frac{3(4\pi)^2 \alpha_e^2}{8G_F^2} \left[|A_{ND}|^2 + |A_D|^2 \left(\frac{16}{3} \log \left(\frac{m_i}{m_j} \right) - \frac{22}{3} \right) \right. \\
&\quad + \frac{1}{6} |B|^2 + \frac{1}{3} \frac{m_i^2 m_j^2 (3 \sin^4 \theta_W - \sin^2 \theta_W + \frac{1}{4})}{m_W^4 \sin^4 \theta_W} |A_D|^2 \\
&\quad \left. + \left(-2A_{ND}A_D^* + \frac{1}{3}A_{ND}B^* - \frac{2}{3}A_DB^* + \text{h.c.} \right) \right] \\
&\quad \times \mathcal{B}(l_i \rightarrow l_j \nu_i \bar{\nu}_j), \tag{29}
\end{aligned}$$

where α_e is the fine structure constant. A_D is the dipole contribution,

$$A_D = \frac{g_j^* g_i F(x)}{2(4\pi)^2 m_{H^\pm}^2}, \tag{30}$$

with $g_{i,j}$ the couplings, m_{H^\pm} the mass of heavy Higgs (H^\pm) and $x = \frac{m_{iR}^2}{m_{H^\pm}^2}$. Expression of $F(x)$ will given shortly. The coefficients A_{ND} and B are the non-dipole contributions from

the penguin and the box diagrams, respectively, which read

$$A_{ND} = \frac{g_j^* g_i}{6(4\pi)^2 m_{H^\pm}^2} G(x), \quad (31)$$

and

$$\begin{aligned} B &= \frac{1}{(4\pi)^2 e^2 m_{H^\pm}^2} \sum_{i,j=1}^3 \left[\frac{1}{2} D_1(x_i, x_j) g_{jj}^* g_{jj} g_{ij}^* g_{ii} + \sqrt{x_i x_j} D_2(x_i, x_j) g_{jj}^* g_{jj}^* g_{ij} g_{ii} \right] \\ &\longrightarrow \frac{1}{(4\pi)^2 e^2 m_{H^\pm}^2} \left[\frac{1}{2} D_1(x) g_j^* g_j g_j^* g_i + x D_2(x) g_j^* g_j^* g_j g_i \right]. \end{aligned} \quad (32)$$

Note that only one flavor of (mediated) neutrino is assumed. So $D_1(x_i, x_j) = D_1(x)$, $D_2(x_i, x_j) = D_2(x)$, and

$$F(x) = \frac{1 - 6x + 3x^2 + 2x^3 - 6x^2 \log x}{6(1-x)^4}, \quad (33)$$

$$G(x) = \frac{2 - 9x + 18x^2 - 11x^3 + 6x^3 \log x}{6(1-x)^4}, \quad (34)$$

$$D_1(x) = \frac{-1 + x^2 - 2x \log x}{(1-x)^3}, \quad (35)$$

$$D_2(x) = \frac{-2 + 2x - (1+x) \log x}{(1-x)^3}, \quad (36)$$

and

$$F(1) = \frac{1}{10}, \quad G(1) = \frac{1}{4}, \quad D_1(1) = \frac{1}{3}, \quad D_2(1) = \frac{1}{6}. \quad (37)$$

With fixed masses for the charged scalar Higgs and the heavy neutrinos, the branching ratio at the one-loop level is shown in Fig.12. We can see that the decay rate is still below the detection sensitivity in Eq.(27) even if we choose the couplings to be $\mathcal{O}(1)$. So new released data can possibly test our predictions. Similar discussions can be given for the same three-body decays mediated by the W boson and the heavy neutrinos at one-loop level. We, however, neglect such contributions since their contributions may be comparably small for the couplings of same size.

V. DISCUSSION AND CONCLUSION

We discuss the possible effects of the new exotic fields H^\pm (together with the right-handed neutrino), H^0 and Z_H^0 in the MTH models on the muon anomaly magnetic moment $g - 2$ and the LFV processes $\ell_i \rightarrow \ell_j \gamma$ and $\ell_i \rightarrow \ell_j \ell_k \ell_l$, respectively.

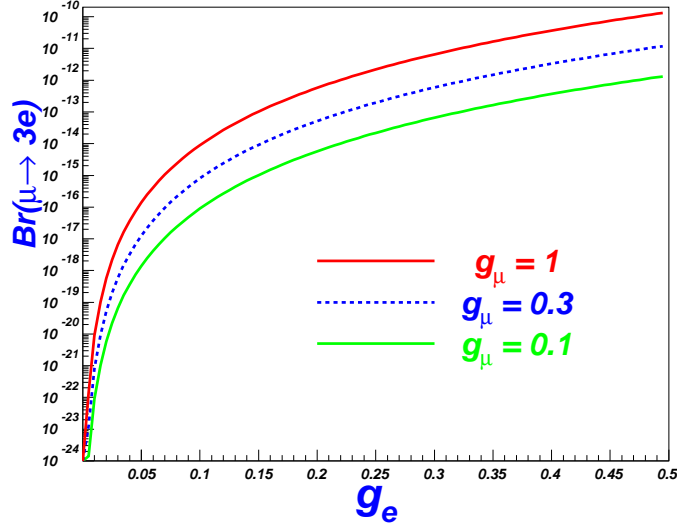


FIG. 12: The branching ratios of $\mu \rightarrow 3e$ at the one-loop level versus parameters g_e with $g_\mu = 0.1, 0.3, 1$, respectively.

From the discussion given above, with the assumption of degenerate heavy neutrino for simplification, we can draw the following conclusions:

- The new contributions from these new particles at one-loop level can not account for the discrepancy of the muon anomalous magnetic moment between the theoretical predictions and the experimental results, since the new contributions are too small in MTH models.
- In most parameter space, the decay channel $\ell_i \rightarrow \ell_j \gamma$ can hardly be probed at current colliders. However, the decay is sensitive to the parameter $V_{e\mu}$, and it can possibly reach the detection sensitivity in some narrow parameters space.
- Similarly, the decay channel $\ell_i \rightarrow \ell_j \ell_k \ell_l$ can hardly be detected at current colliders.

Previous conclusions indicate that the constraints of LFV processes on the parameters of MTH are quite weak. Updated experimental data on LFV processes may shed new light on the discovery potential of MTH models.

Acknowledgments

This work was supported by the National Natural Science Foundation of China(NSFC) under grant 11675147,12075213, 11775012, by the Key Project by the Education Department of Henan Province under grant number 21A140025, by the Fundamental Research Cultiva-

tion Fund for Young Teachers of Zhengzhou University(JC202041040) and the Academic Improvement Project of Zhengzhou University.

- [1] S. L. Glashow, J. Iliopoulos and L. Maiani, Phys. Rev. D 2, 1285 (1970).
- [2] S. Petcov, Sov. J, Nucl. Phys., **25**: 340 (1977).
- [3] J.Chang, K. Cheung, H. Ishida et al, JHEP, **1710**: 039 (2017) arXiv: hep-ph/1707.04374.
- [4] T. A. Chowdhury and S. Nasri, Phys.Rev. D, **97**: 075042 (2018) arXiv: hep-ph/1801.07199.
- [5] J. L. Diaz-Cruz, J. J. Toscano, Phys. Rev. D, **62**: 116005 (2000) arXiv:hep-ph/9910233.
- [6] T. Han, D. Marfatia, Phys. Rev. Lett., **86**: 1442 (2001) arXiv: hep-ph/0008141.
- [7] K. Agashe, R. Contino, Phys. Rev. D, **80**: 075016 (2009) arXiv:hep-ph/0906.1542.
- [8] S. Casagrande et al., JHEP, **10**: 094 (2008) arXiv:hep-ph/0807.4937.
- [9] Guo-Li Liu, Fei Wang, Kuan Xie, Xiao-Fei Guo, Phys. Rev. D96, (2017) 035005, arXiv:1701.00947.
- [10] Jinlei Yang, T. Feng, Y. Yan, Wei Li, S. Zhao, H. Zhang, Phys. Rev. D 99, (2019) 015002, arXiv:1812.03860.
- [11] Xiaofang Han, Tianjun Li, Lei Wang, Yang Zhang, Phys. Rev. D 99, (2019) 095034, arXiv:1812.02449.
- [12] Mario W. Barea, V. Pleitez, Phys. Rev. D 101, (2020) 015024, arXiv:1912.05900.
- [13] Chongxing Yue, Z. Zong, Li Zhou, Shuo Yang, Phys.Rev.D71, (2005) 115011, arXiv:hep-ph/0506070.
- [14] Junjie Cao, Zhaohua Xiong, Jin Min Yang, Eur.Phys.J. C32, (2004) 245, arXiv:hep-ph/0307126.
- [15] Deirdre Black, Tao Han, Hong-Jian He, Marc Sher, Phys.Rev.D66, (2002) 053002, arXiv:hep-ph/0206056.
- [16] J. P. Miller, E. de Rafael, and B. L. Roberts, Rept. Prog. Phys. 70, 795 (2007), arXiv:hep-ph/0703049.
- [17] F. Jegerlehner and A. Nyffeler, Phys. Rept. 477, 1 (2009), arXiv:0902.3360.
- [18] J. P. Miller, E. de Rafael, B. L. Roberts, and D. Stckinger, Annu. Rev. Nucl. Part. Sci. 62, 237 (2012).

- [19] M. Lindner, M. Platscher, and F. S. Queiroz, *Phys. Rept.* **731**, 1 (2018), arXiv:1610.06587.
- [20] F. Jegerlehner, *Springer Tracts Mod. Phys.* **274**, pp.1 (2017).
- [21] Guo-Li Liu, Qing-Guo Zeng, *Euro. Phys. J. C* **79**, (2019) 612, arXiv:1811.04777.
- [22] K. Abe et al (T2K Collab), *Phys. Rev. Lett.*, **107**: 041801 (2011).
- [23] P. Adamson et al (MINOS Collab), *Phys. Rev. Lett.*, **107**: 181802 (2011).
- [24] Y. Abe et al (DOUBLE-CHOOZ Collab), *Phys. Rev. Lett.*, **108**: 131801 (2012).
- [25] F. An et al (DAYA-BAY Collab), *Phys. Rev. Lett.*, **108**: 171803 (2012).
- [26] J. Ahn et al (RENO Collaboration), *Phys. Rev. Lett.*, **108**: 191802 (2012).
- [27] P. Ghosh, S. Roy, *JHEP*, **0904**: 069 (2009).
- [28] M. C. Gonzalez-Garcia and M. Maltoni, *Phys. Rep.*, **460**: 1 (2008).
- [29] M. C. Gonzalez-Garcia, M. Maltoni, J. Salvado and T. Schwetz, *JHEP*, **1212**: 123 (2012).
- [30] I. Girardi, S. T. Petcov, A. V. Titov, *Nucl. Phys. B*, **894**: 733-768 (2015).
- [31] P. Minkowski, *Phys. Lett.* **67B** (1977)421;
R. N. Mohapatra and G. Senjanovic, *Phys. Rev. Lett.* **44** (1980) 912;
T. Yanagida, *Conf. Proc. C7902131* (1979)95;
M. Gell-Mann, P. Ramond, and R. Slansky, *Conf. Proc. C790927* (1979) 315.
- [32] M. Magg and C. Wetterich, *Phys. Lett. B* **94** (1980) 61;
J. Schechter and J. W. F. Valle, *Phys. Rev. D* **22** (1980) 2227;
C. Wetterich, *Nucl. Phys. B* **187** (1981) 343;
G. Lazarides, Q. Shafi, and C. Wetterich, *Nucl. Phys. B* **181** (1981) 287;
R. N. Mohapatra and G. Senjanovic, *Phys. Rev. D* **23** (1981) 165.
- [33] R. Foot, H. Lew, X. G. He, and G. C. Joshi, *Z. Phys. C* **44** (1989) 441;
E. Ma, *Phys. Rev. Lett.* **81** (1998) 1171;
E. Ma and D. P. Roy, *Nucl. Phys. B* **644** (2002) 290.
- [34] Z. Chacko, H.-S. Goh, and R. Harnik, *Phys. Rev. Lett.* **96**, 231802 (2006), arXiv:hep-ph/0506256 [hep-ph].
- [35] ATLAS Collaboration, M. Aaboud et al., *Phys. Rev. D* **98** (2018), no. 3, 032008, arXiv:1803.10178; CMS Collaboration, A. M. Sirunyan et al., *JHEP* **05** (2018) 025, arXiv:1802.02110; ATLAS Collaboration, G. Aad et al., *Phys. Lett. B* **758** (2016) 249-268, arXiv:1602.06034; CMS Collaboration, A. M. Sirunyan et al., *JHEP* **08** (2018) 177, arXiv:1805.04758.

- [36] P. F. de Salas and S. Pastor, "Relic neutrino decoupling with flavour oscillations revisited", JCAP 1607 (2016), no. 07, 051, arXiv:1606.06986.
- [37] G. Mangano, G. Miele, S. Pastor, and M. Peloso, "A Precision calculation of the effective number of cosmological neutrinos", Phys. Lett. B534 (2002) 8-16, arXiv:astro-ph/0111408.
- [38] Z. Chacko, N. Craig, P. J. Fox, and R. Harnik, JHEP 07 (2017) 023, arXiv:1611.07975.
- [39] R. H. Cyburt, B. D. Fields, K. A. Olive, and T.-H. Yeh, Rev. Mod. Phys. 88 (2016) 015004, arXiv:1505.01076. "Big Bang Nucleosynthesis: 2015",
- [40] Planck Collaboration, N. Aghanim et al., arXiv:1807.06209.
- [41] N. Craig, A. Katz, M. Strassler, and R. Sundrum, JHEP 07 (2015)105, arXiv:1501.05310.
- [42] R. Barbieri, L. J. Hall, and K. Harigaya, JHEP 11 (2016) 172, arXiv:1609.05589.
- [43] C. Csaki, E. Kuflik, and S. Lombardo, Phys. Rev. D96 (2017), no. 5, 055013, arXiv:1703.06884.
- [44] B. Batell and C. B. Verhaaren, arXiv:1904.10468.
- [45] D. Liu and N. Weiner, arXiv:1905.00861.
- [46] N. Craig, S. Koren, and T. Trott, JHEP 05 (2017) 038, arXiv:1611.07977.
- [47] N. Craig, S. Knapen, P. Longhi, and M. Strassler, JHEP 07 (2016) 002, arXiv:1601.07181.
- [48] Csaba Csaki, Eric Kuflik, Salvator Lombardo, Phys. Rev. D 96, 055013 (2017), arXiv:1703.06884 [hep-ph].
- [49] Zackaria Chacko, Nathaniel Craig, Patrick J. Fox, Roni Harnik, Report number: FERMILAB-PUB-16-555-T, arXiv:1611.07975 [hep-ph].
- [50] Yang Bai, Ran Lu, Sida Lu, Jordi Salvado, Ben A. Stefanek, Phys. Rev. D 93, 073004 (2016), arXiv:1512.05357.
- [51] W. Emam and S. Khalil, Eur. Phys. J. C **55**, 625 (2007), [arXiv:0704.1395 [hep-ph]].
- [52] W. Abdallah, A. Awad, S. Khalil, H. Okada, Eur. Phys. J. C 72(2012)2108, arXiv:1105.1047 [hep-ph].
- [53] Z. Maki, M. Nakagawa and S. Sakata, Prog. Theor. Phys. **28**, 870 (1962).
- [54] A.G. Akeroyd (Taiwan, Natl. Cheng Kung U.), Mayumi Aoki (Tokyo U., ICRR), Hiroaki Sugiyama, Phys.Rev.D77:075010,2008, arXiv:0712.4019 [hep-ph].
- [55] S. Antusch, C. Biggio, E. Fernandez-Martinez, M. B. Gavela and J. Lopez-Pavon, JHEP 0610, 084 (2006) [arXiv:hep-ph/0607020]; M. Malinsky, T. Ohlsson, Z. z. Xing and H. Zhang, Phys. Lett. B 679, 242 (2009) [arXiv:0905.2889 [hep-ph]]; A. Ibarra, E. Molinaro and S. T. Petcov, arXiv:1103.6217 [hep-ph].

- [56] G. W. Bennett et al, [Muon g-2 Collaboration], Phys. Rev. D **73** (2006)072003.
- [57] F. Jegerlehner and R. Szafron, Eur.Phys.J.C71:1515 (2011)[arXiv:1101.2872 [hep-ph]].
- [58] M. Davier, A. Hoecker, B. Malaescu and Z. Zhang, Eur.Phys.J.C71:1515 (2011)[arXiv:1010.4180 [hep-ph]].
- [59] T. Hahn, M. Perez-Victoria, Comput. Phys. Commun. 118 (1999) 153 [hep-ph/9807565].
T. Hahn, Nucl. Phys. Proc. Suppl. 89 (2000) 231, hep-ph/0005029; ibid.135 (2004) 333, hep-ph/0406288; hep-ph/0408247. G. 't Hooft and M. Veltman, Nucl. Phys. B153 (1979) 365.
- [60] A. M. Baldini et al., MEG Collaboration, Eur. Phys. J. C76,(2016) 434, arXiv:1605.05081 [hep-ex].
- [61] J. Adam et al., MEG Collaboration, Phys. Rev. Lett. 107, 171801 (2011), arXiv:1107.5547 [hep-ex].
- [62] Antonio Pich, Report. No: IFIC/13-79, FTUV/13-1028, arXiv:1310.7922 [hep-ph].
- [63] [21] B. Aubert et al. [BABAR Collaboration], Phys. Rev. Lett.104, (2010) 021802. [arXiv:0908.2381 [hep-ex]].
- [64] M. Tanabashi et al., , Particle Data Group Collaboration, Phys. Rev. D98,(2018) 030001.
- [65] K. Hayasaka, et al.(Belle collaboration), Phys. Lett. B687, 139 (2010) [arXiv:1001.3221 [hepex]].
- [66] Meziane Chekkal, Amine Ahriche, Amine Bouziane Hammou, Salah Nasri, Phys. Rev. D95, (2017) 095025, arXiv:1702.04399 [hep-ph].
- [67] Subhasmita Mishra, Anjan Giri, arXiv:1909.12147 [hep-ph].